

Article

# Green Corrosion Inhibition of Mild Steel by Hydrazone Derivatives in 1.0 M HCl

Abdelkarim Chaouiki <sup>1</sup>, Maryam Chafiq <sup>1</sup>, Hassane Lgaz <sup>2,\*</sup>, Mustafa R. Al-Hadeethi <sup>3</sup>, Ismat H. Ali <sup>4</sup> , Sheerin Masroor <sup>5</sup> and Ill-Min Chung <sup>2,\*</sup>

<sup>1</sup> Laboratory of Applied Chemistry and Environment, ENSA, University Ibn Zohr, PO Box 1136, Agadir 80000, Morocco; abdelkarim.chaouiki@uit.ac.ma (A.C.); maryam.chafiq@edu.uiz.ac.ma (M.C.)

<sup>2</sup> Department of Crop Science, College of Sanghur Life Science, Konkuk University, Seoul 05029, Korea

<sup>3</sup> Department of Chemistry, College of Education, Kirkuk University, Kirkuk 36001, Iraq; mustfaa70@yahoo.com

<sup>4</sup> Department of Chemistry, College of Science, King Khalid University, P.O. Box 9004, 61413 Abha, Saudi Arabia; ismathassanali@gmail.com

<sup>5</sup> Department of Chemistry, Anugrah Narayan College, Patliputra University, Patna 800013, Bihar, India; masroor.sheerin@gmail.com

\* Correspondence: hlgaz@konkuk.ac.kr (H.L.); imcim@konkuk.ac.kr (I.-M.C.)

Received: 29 May 2020; Accepted: 29 June 2020; Published: 30 June 2020



**Abstract:** In the present study, the inhibition performance of two synthesized hydrazone derivatives (HDZs), namely, (E)-N'-(2,4-dimethoxybenzylidene)-2-(6-methoxynaphthalen-2-yl) propanehydrazide (HYD-1) and N'-cyclohexylidene-2-(6-methoxynaphthalen-2-yl) propanehydrazide (HYD-2) on mild steel (MS) in 1.0 M HCl was investigated using weight loss measurements, electrochemical techniques, and scanning electron microscope (SEM) coupled with energy-dispersive X-ray spectroscopy (EDX). The experimental data suggested that the hydrazone derivatives exhibited a high inhibition performance, which increases with increasing their concentrations. HYD-1 and HYD-2 presented maximum inhibition efficiencies of 96% and 84%, respectively, at an optimal concentration of  $5 \times 10^{-3}$  M. The principal observations that resulted from electrochemical studies are that HYDs affected both anodic and cathodic reactions (mixed inhibitors). Their adsorption, which is a combination of chemisorption and physisorption, obeyed the Langmuir isotherm model. Furthermore, the temperature effect was carried out at various temperatures ranging from 303 to 333 K to verify the corrosion inhibition performance of HYD-1 at higher temperatures. Moreover, SEM-EDX analysis confirmed that HYDs can ensure remarkable prevention against corrosion through the adsorption onto the metal surface.

**Keywords:** corrosion inhibitor; mild steel; electrochemical; hydrazone derivative; SEM-EDX analysis

## 1. Introduction

It is well known that acid solutions, especially hydrochloric acid, used for the removal of undesirable scale and rust in metal finishing industries, oil-well acidizing in oil recovery, cleaning of boilers, etc., trigger corrosion of pure metals and alloys [1]. Mild steel is a familiar material used in many industrial applications, especially in petroleum production units [2]. The use of hydrochloric acid solutions for maximizing the initial productivity of new wells or restore it for aging wells causes severe corrosion to the equipment [3]. Therefore, investments in protective measures should be required to prevent the metal loss due to corrosion. It is now well established from a variety of studies that organic compounds containing heteroatoms such as N, S, P, and O, functional groups,  $\pi$ -bonds, and aromatic heterocyclic rings play a vital role in the inhibition and mitigation of corrosion in acidic environments [4,5]. Organic compounds with these specific elements in their molecular structures

could be useful corrosion inhibitors [6,7]. They can adsorb on the metal surface to form protective layers that separate the mild steel surface from hydrochloric acid and thereby reducing the corrosion rate, which prevents mild steel degradation.

Moreover, heterocyclic functional groups that play a significant role in increasing the surface coverage could also increase the solubility of organic compounds in the aggressive environment (e.g., HCl). However, the toxicity of some organic corrosion inhibitors has compelled the search for organic compounds, containing heteroatoms and/or a long carbon chain in their molecular structures and having promising properties like low cost, biodegradability, and non-toxicity [8]. In the corrosion inhibition field, such compounds are generally called 'green corrosion inhibitors'.

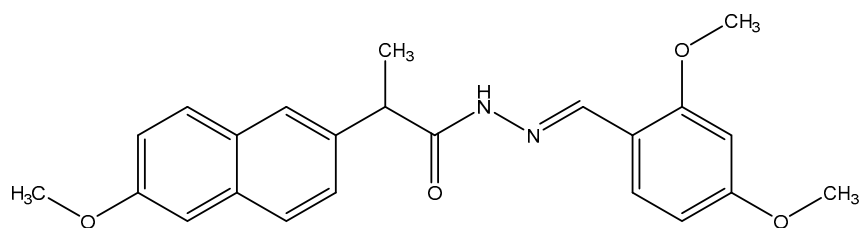
More recently, our research group contributed to the development of a particular class of organic compounds based on hydrazones, spirocyclopropanes, pyrazolines, quinolines, benzodiazepines, chalcones, etc., which have been the subject of many studies and publications [3,9–13]. To continue these ongoing efforts and to develop new effective corrosion inhibitors, two hydrazone derivatives based on Naproxen have been developed and evaluated as corrosion inhibitors for mild steel (MS) in 1.0 M HCl medium. Naproxen is one of the most regularly used propionic acid derivatives for the treatment of pain, joint swelling, and symptoms of arthritis. It is believed to work by blocking the action of cyclooxygenase (COX) involved in the production of prostaglandins that are produced in response to injury or certain diseases and cause pain, swelling, and inflammation. However, its use is associated with some gastrointestinal side effects possibly caused by its acidic group [14]. One of the easier and safer ways to functionalize the carboxylate group is its functionalization into hydrazones [15]. Hydrazones are a class of organic compounds characterized by the azomethine bond  $R_1R_2C=NHNH_2$ , where  $R_1$ ,  $R_2$  can be a different functional group, so that hydrazones represent essential starting materials in organic synthesis in addition to their biological importance [16,17]. The primary reason for choosing (E)-N'-(2,4-dimethoxybenzylidene)-2-(6-methoxynaphthalen-2-yl)propanehydrazide (HYD-1) and N'-cyclohexylidene-2-(6-methoxynaphthalen-2-yl)propanehydrazide (HYD-2) compounds, besides their eco-friendly character, is their molecular structures. They are comprised of a combination of aromatic rings, imine functionality ( $-C=N-$ ), acyl group, electron-donating groups like methoxy ( $-OCH_3$ ) and methyl ( $-CH_3$ ), and more than one conjugated system containing nitrogen and oxygen atoms. Hence, they could be interesting compounds for protecting metal substrate in the acidic medium. To confirm our assumptions, corrosion inhibition performances of the two studied compounds were examined using potentiodynamic polarization (PDP) and electrochemical impedance spectroscopy (EIS) methods as well as weight loss (WL). In addition, further experimental investigations were performed to evaluate the effect of immersion time and temperature on the inhibition efficiency. Furthermore, the inhibition effect of the target inhibitors was also investigated through the morphological characterization of the mild steel substrates by scanning electron microscope/energy-dispersive X-ray spectroscopy (SEM/EDX) analysis.

## 2. Experimental Procedures

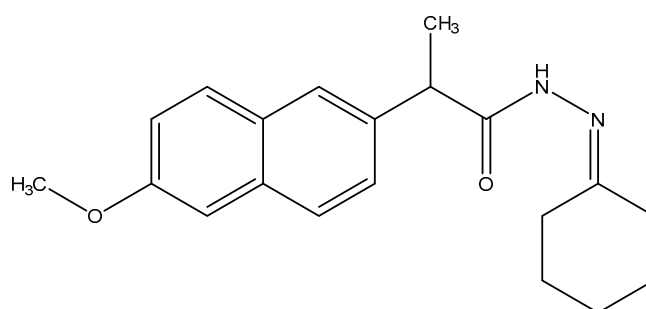
### 2.1. Materials and Electrolytes

The metal used for all experimental tests is a mild steel with the following chemical composition (in wt %): Fe (99.21%), C (0.21%), Si (0.38%), Mn (0.05%), S (0.05%), P (0.09%), and Al (0.01%). The 1.0 M HCl was prepared by diluting the analytical grade of 37% hydrochloric acid solution (Sigma-Aldrich) with double-distilled water. First of all, MS samples were mechanically polished using a rotating disc containing 400, 800, 1200, and 1600 grit emery papers. Next, the samples were degreased in acetone, rinsed using distilled water, dried in a hot air blower, and finally transferred immediately to experimental tests. In the present research, we prepared four test solutions with a concentration range of  $1 \times 10^{-4}$  to  $5 \times 10^{-3}$  M to examine the influence of HYD-1 and HYD-2 compounds on mild steel (MS) corrosion. Figure 1 shows the molecular structure of the tested compounds along with their chemical

name and abbreviation. The full synthesis and characterization details of both compounds are given in Supplementary Materials.



(E)-N'-(2,4-dimethoxybenzylidene)-2-(6-methoxynaphthalen-2-yl)propanehydrazide (**HYD-1**)



N'-cyclohexylidene-2-(6-methoxynaphthalen-2-yl)propanehydrazide (**HYD-2**)

**Figure 1.** Molecular structures of (E)-N'-(2,4-dimethoxybenzylidene)-2-(6-methoxynaphthalen-2-yl)propanehydrazide (HYD-1) and N'-cyclohexylidene-2-(6-methoxynaphthalen-2-yl)propanehydrazide (HYD-2).

## 2.2. Weight Loss (WL) Study

Weight loss (WL) measurements were carried out in a stagnant aerated solution of 1.0 M HCl. For this study, we choose the mild steel (MS) rectangular substrates with dimensions of 2.5 cm × 2 cm × 0.9 cm. As previously stated, before each experiment, samples were prepared and thoroughly cleaned. During all gravimetric tests, the MS samples were weighed with a precision balance (precise to 0.1 mg) and then immersed in corrosion solutions in the absence and the presence of the compounds under study for an immersion period of 24 h at a temperature range from 303 to 333 K ± 2 K. Experiments described here were repeated three times to confirm the results, and only the average values were considered. After attaining 24 h of immersion time, the specimens were taken out, cleaned thoroughly with distilled water and acetone, dried in air, and precisely weighed again. All experimental methodologies based on weight loss measures and MS specimens preparation were carried out under the ASTM standard conditions [18]. The weight difference before and after immersion in test solutions is estimated and represented by  $W$  (in gram) to calculate the corrosion rate ( $C_{RW}$  in  $\text{mg cm}^{-2} \text{h}^{-1}$ ) by the following Equation (1):

$$C_{RW} = \frac{K \times W}{A \times t \times \rho} \quad (1)$$

For  $K$ ,  $A$ , and  $\rho$  parameters under the standard condition of ASTM;  $K$  was used as constant and equal to  $8.76 \times 10^4$ ,  $A$  is the exposed MS area in  $\text{cm}^2$  and  $\rho$  (density) =  $7.86 \text{ g cm}^{-3}$ , and  $t$  denotes immersion time in hours.

The corrosion inhibition efficiency of tested compounds and their degree of surface coverage ( $\theta$ ) were determined using the average mass loss, as given below by Equations (2) and (3) [19,20]:

$$\eta_{WL}(\%) = \left[ \frac{C_{RW}^o - C_{RW}^{HYD}}{C_R^o} \right] \times 100 \quad (2)$$

$$\theta = \frac{\eta_{WL}}{100} \quad (3)$$

where  $C_{RW}^o$  and  $C_{RW}^{HYD}$  correspond to corrosion rates of the mild steel in blank solution and after the addition of different concentrations of HYDs derivatives, respectively.

### 2.3. Electrochemical Measurements for Corrosion Inhibition

Electrochemical measurements have emerged as powerful techniques in studying and evaluating the corrosion behavior of mild steel. All electrochemical tests were conducted in a corrosion cell with three different functional electrodes. The MS is used as working electrode which has a surface area of 1 cm<sup>2</sup>, the saturated calomel electrode (SCE) was used as the reference electrode, and the platinum (Pt) electrode served as the counter electrode. Electrochemical tests were performed using Wuhan Corrtest Instruments Corp., Ltd., (Wuhan, China), controlled with a computer and the electrochemical data were acquired using an electrochemical analyzer software. The mild steel electrode has been soaked in a cell containing 80 mL of the acid solution, i.e., 1.0 M HCl solution with a concentration range of  $1 \times 10^{-4}$  to  $5 \times 10^{-3}$  M.

Moreover, the electrochemical experiments were run after 30 min at  $303 \text{ K} \pm 2 \text{ K}$  to acquire a relatively stable value obtained by the open circuit potential (OCP). For the electrochemical characterization of mild steel by PDP tests, the electrode potential was recorded automatically from  $-700$  to  $-300$  mV versus SCE at steady open-circuit potential, and a scan rate was set at 0.5 mV/s. The EIS tests were done at premeasured OCP by superimposing a sinusoidal AC potential perturbation of 5 mV in the frequency range of 10 mHz to 100 kHz. Once the PDP curves were extracted, the electrochemical parameters were estimated from Tafel plots with the aid of the Tafel extrapolation method. Furthermore, the EC lab software (V10.34) was applied to analyze EIS data.

### 2.4. Surface Characterization (SEM/EDX)

The morphological characterization of the MS surface was performed using the scanning electron microscope coupled with the EDX analyzer (JEOL Ltd., Tokyo, Japan). Effects of studied molecules added to the acid solution on MS corrosion were assessed by taking photographs immediately after 24 h of immersion in uninhibited and inhibited acidic medium. Meanwhile, the elemental constituents of layers formed on MS were recorded and examined using EDX analysis.

## 3. Results and Discussion

### 3.1. Comparison of Inhibition Performances Using Weight Loss Strategy

#### 3.1.1. Influence of Inhibitors Concentrations

The effect of inhibitors concentrations on the corrosion rate of mild steel was primarily studied in the blank solution and in a solution containing different concentrations of studied hydrazone derivatives using the weight loss technique. The inhibition efficiencies and the corrosion rate values were calculated and compared for both compounds, i.e., HYD-1 and HYD-2, at various concentrations for 24 h of immersion at  $303 \text{ K} \pm 2 \text{ K}$ , and the obtained results are graphically summarized in Figure 2. As can be seen from this figure, the corrosion rate of mild steel is decreased by increasing the amount of HYDs compared to the blank solution. Moreover, from these results, we can see a growing trend towards the rise in the inhibition efficiency with the increase in the concentration of HYDs—it reached

a maximum value of 95% for HYD-1 and 86% for HYD-2 at  $5 \times 10^{-3}$  M, as revealed in Figure 2. The presented results provide evidence that when inhibitors were added, the surface area coverage of MS is significantly increased and the protective effect of the inhibitor's film is greatly enhanced, thus reducing the mild steel corrosion rate. Interestingly, there are also differences in the inhibition efficiency of inhibitors. The HYD-1 inhibitor was observed to be the effective compound against steel corrosion in the 1.0 M HCl solution compared to HYD-2. These differences in inhibitory efficacies can be explained by several factors. From these preliminary results obtained by a gravimetric study, a possible explanation for the better performance of HYD-1 is that it contains powerful functional groups like methoxy groups, acyl groups, as well as the length of the carbon chain, which promote its adsorption onto the mild steel surface. Briefly, it can be inferred that the two inhibitor molecules can be adsorbed easily onto the metal surface [3].

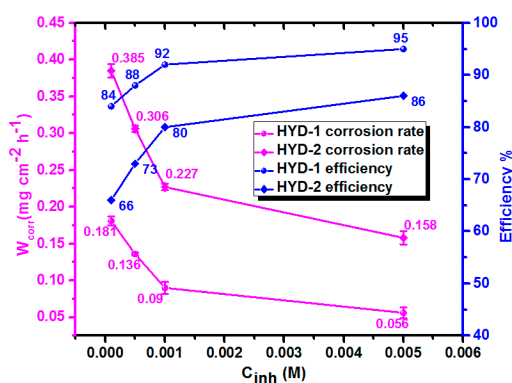


**Figure 2.** The variation of corrosion rate and protection efficiency with the HYD-1 and HYD-2 concentrations for mild steel in 1.0 M HCl at 303 K.

### 3.1.2. Influence of the Temperature on Inhibitor Performances

In parallel to the concentration effect, a temperature effect study was performed to further examine and give more insight into the stability of inhibitor molecules under higher temperatures taking into consideration the wide range of applications of mild steel. This part discusses the findings obtained from weight loss measurements carried out at various temperatures ranging from 303 K to 333 K. The effect of temperature on MS dissolution in terms of corrosion rate in 1.0 M HCl was evaluated in the absence and presence of various concentrations of HYD-1. The temperature impact on the corrosion rate and effectiveness of HYD-1 is inserted in Table 1, while Table 2 provides thermodynamic parameters related to the temperature effect computed from analyzing the Arrhenius plots.

From the data in Table 1, it is apparent that with the rise in temperature, the surface shows high corrosion rate values accompanied with a decrease in the protectiveness of HYD-1. Further, the decline in the inhibition efficiency of HYD-1 at higher temperatures may be mainly interpreted by acid-catalyzed molecular fragmentation or hydrolysis of the studied inhibitor at high temperatures [21,22]. However, what can be seen in Table 1 is that the decrease in the protection efficiency of HYD-1 is insignificant; from 95% (303 K,  $5 \times 10^{-3}$  M) to 81% (333 K,  $1 \times 10^{-4}$  M). It indicates that the adsorption of the HYD-1 compound on the MS surface is stable even at a higher temperature, and thus, effective protection can be assured at those conditions. Furthermore, this relationship between the effect of temperature and tendency of the adsorption of the inhibitor can be best explained by the Arrhenius equation and the transition state functions to give a qualitative picture of studied inhibitors in the HCl medium.

Arrhenius curves were fitted to determine the thermodynamic parameters such as enthalpy change of activation ( $\Delta H^*$ ), entropy change ( $\Delta S^*$ ), and activation energy ( $E_a$ ) for the mild steel corrosion in 1.0 M HCl without and with different concentrations of HYD compounds using the following equations:

$$C_{WL} = K \times e^{\frac{-E_a}{RT}} \quad (4)$$

$$C_{WL} = \frac{RT}{Nh} \exp\left(\frac{\Delta S^*}{R}\right) \exp\left(\frac{\Delta H^*}{RT}\right) \quad (5)$$

where  $K$  denotes the pre-exponential factor,  $h$  signifies the Planck constant,  $N$  denotes the number of Avogadro,  $R$  is the universal gas constant, and  $T$  represents the temperature.

**Table 1.** Influence of temperature toward the corrosion rate ( $\pm$ SD) and inhibition efficiency for mild steel in 1.0 M HCl with and without the HYD-1 compound.

Solution	Concentration	Temperature	Corrosion Rate	$\eta_{WL}$
		K	mg/cm <sup>2</sup> × h	%
Blank	1.0 M HCl	303	1.135 ± 0.0121	-
		313	1.416 ± 0.0215	-
		323	1.998 ± 0.0214	-
		333	2.539 ± 0.0316	-
HYD-1	1 × 10 <sup>-4</sup>	303	0.181 ± 0.0060	84
		313	0.240 ± 0.0075	83
		323	0.359 ± 0.0065	82
		333	0.482 ± 0.0044	81
	5 × 10 <sup>-4</sup>	303	0.136 ± 0.0021	88
		313	0.184 ± 0.0010	87
		323	0.279 ± 0.0073	86
		333	0.380 ± 0.0088	85
	1 × 10 <sup>-3</sup>	303	0.090 ± 0.0080	92
		313	0.127 ± 0.0045	91
		323	0.199 ± 0.0081	90
		333	0.279 ± 0.0031	89
5 × 10 <sup>-3</sup>	303	0.056 ± 0.0075	95	
	313	0.099 ± 0.0034	93	
	323	0.159 ± 0.0084	92	
	333	0.228 ± 0.0052	91	

**Table 2.** Thermodynamic activation parameters for the mild steel (MS) electrode in 1.0 M HCl in the presence and absence of different concentrations of HYD-1.

Parameters	$E_a$ (kJ mol <sup>-1</sup> )	$\Delta H^*$ (kJ mol <sup>-1</sup> )	$\Delta S^*$ (J mol <sup>-1</sup> K <sup>-1</sup> )	$(E_a - \Delta H^*)$ (kJ mol <sup>-1</sup> )	
Blank	23.12	20.48	-176.48	2.64	
HYD-1	1 × 10 <sup>-4</sup>	28	25.36	-175.66	2.64
	5 × 10 <sup>-4</sup>	29.32	26.68	-173.65	2.64
	1 × 10 <sup>-3</sup>	32.22	29.58	-167.51	2.64
	5 × 10 <sup>-3</sup>	39.39	36.75	-147.32	2.64

The kinetic activation parameters derived from Arrhenius and transition state plots, shown in Figure 3a,b, are listed in Table 2.

As shown in Table 2, the values of activation energy ( $E_a$ ) are generally seen as a factor strongly related to the concentration of inhibitors, and all  $E_a$  values calculated for inhibited systems are greater than those of the blank acid solution. The higher value of  $E_a$  in the presence of different concentrations of HYD-1 when compared to the uninhibited system ( $E_a = 23.12$  kJ mol<sup>-1</sup>), suggests that the dissolution of mild steel becomes difficult in the presence of the HYD-1 inhibitor because the energy barrier

was higher. Therefore, a protective film on the surface of MS could be formed [10,23]. Moreover, it is apparent from Table 2 that the enthalpy values increase compared to the uninhibited case and are positive, which indicate the endothermic nature of mild steel dissolution during the corrosion process [24,25]. In terms of the disordering of the molecule during the inhibition process, the high negative values of  $\Delta S^*$  in comparison to the blank solution indicate that there is a decrease in the disorder during the switch from reagents to the activated complex. Furthermore, these findings might be a result of the adsorption of the activated compound which prefers the association rather than dissociation on the MS surface. This is a quasi-substitution phenomenon between inhibitor molecules in the acidic solution and  $H_2O$  molecules present at the MS/electrolyte interface [6,26]. In addition, the obtained results (Table 2) indicate that there is a perfect relationship between  $E_a$  and  $\Delta H^*$  values, which further confirm and validate all these observations.

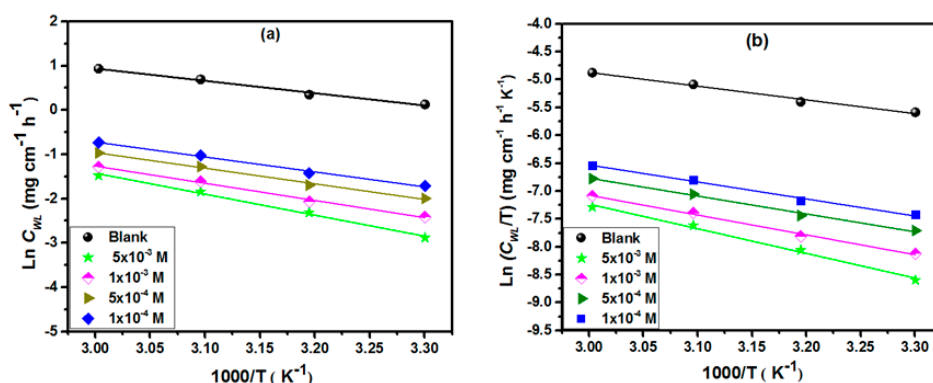


**Figure 3.** Arrhenius (a) and transition state (b) plots of the corrosion rate for mild steel dissolution in 1.0 M HCl solution in the absence and presence of different concentrations of HYD-1.

### 3.2. Potentiodynamic Polarization (PDP) Measurements

The characterization of mild steel explored by relationships between the free corrosion current density and free corrosion potential is essential for understanding the reactions occurring on the mild steel surface. For this purpose, the PDP study was performed in detail to offer some important insights into the kinetics of the anodic and cathodic reactions of the corrosion process. PDP plots of MS coupons immersed in HCl solution in the absence and presence of different concentrations of hydrazone derivatives were carried out after 30 min of immersion time in the acid solution. Figure 4 shows the polarization curves obtained for two studied inhibitors. At the same time, Table 3 summarizes the calculated data from Tafel plots, including free corrosion potential ( $E_{\text{corr}}$ ) and free corrosion current density ( $i_{\text{corr}}$ ), as well as cathodic and anodic Tafel slopes ( $\beta_c$ ,  $\beta_a$ ). According to the calculated values of free corrosion current density, the inhibition efficiency was estimated by using the following equation:

$$E_{\text{PDP}}(\%) = \left[ 1 - \frac{i_{\text{corr}}^{\text{HYD}}}{i_{\text{corr}}^{\text{o}}} \right] \times 100 \quad (6)$$

where  $i_{\text{corr}}^{\text{o}}$  and  $i_{\text{corr}}^{\text{HYD}}$  represent the corrosion current densities, respectively, without and with the addition of different concentrations of hydrazones.

From the data in the table of Section 3.3.2, it can be seen that the presence of two compounds significantly shifted the current densities at OCP (open circuit potential) to lower values, which means that the mild steel corrosion is strongly inhibited after the addition of these inhibitors. Moreover, we can observe that with the increase in inhibitor concentrations, the corresponding protective effectiveness of HYD-1 and HYD-2 increases considerably. The corrosion inhibition efficiency reaches 94% for HYD-1 and 84% for HYD-2 when the dosage of both compounds is  $5 \times 10^{-3}$  M. Furthermore, consistent with the literature, inhibitors molecules may be categorized as an anodic, cathodic, or mixed type based on the deviation in  $E_{\text{corr}}$  regarding the blank acid solution. If the displacement of  $E_{\text{corr}}$  values in absence

and presence of inhibitors is higher than 85 mV, inhibitor molecules are generally categorized as a cathodic or anodic type while those with a displacement of  $E_{\text{corr}}$  lower than 85 mV are considered as mixed-type inhibitors [27,28]. From Figure 4, there is no significant shift in free corrosion potential values, and the displacement in  $E_{\text{corr}}$  between the blank solution and the solution containing inhibitors is only 10 mV and 15 mV for HYD-1 and HYD-2, respectively; less than 85 mV. This finding suggests that the effect of the corrosion inhibition by studied compounds is typically mixed, i.e., affects both cathodic and anodic reactions. Moreover, there was no remarkable variation in anodic and cathodic Tafel slopes (Table 3) in the presence of HYDs, which further confirms that anodic and cathodic reactions occur without modification in their mechanisms [9,29].

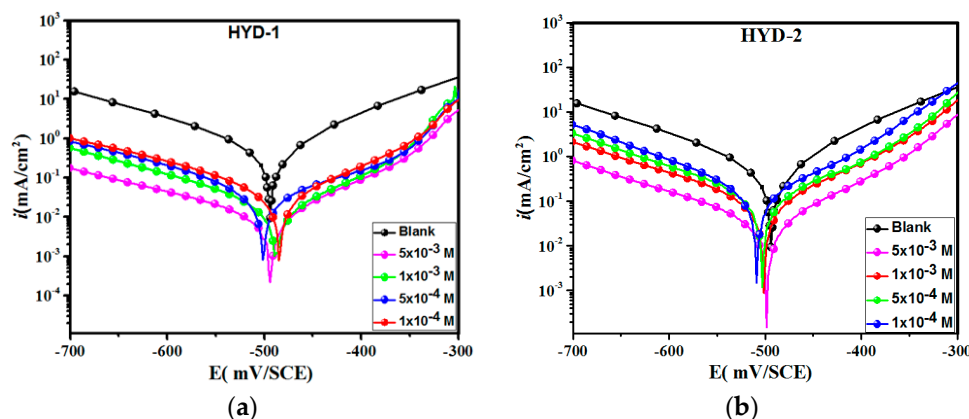


**Figure 4.** Potentiodynamic polarization curves for mild steel in hydrochloric acid solution with and without HYDs at 303 K, (a) HYD-1 and (b) HYD-2.

**Table 3.** Electrochemical parameters derived after extrapolating the inhibited and uninhibited polarization curves.

Inhibitor	Concentration (M)	$-E_{\text{corr}}$ (mV vs. SCE)	$-\beta_c$ (mV dec $^{-1}$ )	$\beta_a$ (mV dec $^{-1}$ )	$i_{\text{corr}}$ ( $\mu\text{A cm}^{-2}$ )	$E_{\text{PDP}}$ (%)
Blank	1.0	496 $\pm$ 0.4	150 $\pm$ 3.5	92 $\pm$ 5.7	564 $\pm$ 2.3	-
HYD-1	1 $\times$ 10 $^{-4}$	486 $\pm$ 0.7	155 $\pm$ 6.8	78 $\pm$ 4.1	82 $\pm$ 6.1	85
	5 $\times$ 10 $^{-4}$	503 $\pm$ 0.4	157 $\pm$ 2.6	64 $\pm$ 3.4	68 $\pm$ 5.3	87
	1 $\times$ 10 $^{-3}$	490 $\pm$ 0.2	139 $\pm$ 2.8	68 $\pm$ 4.9	55 $\pm$ 3.4	90
	5 $\times$ 10 $^{-3}$	494 $\pm$ 0.5	142 $\pm$ 4.8	98 $\pm$ 6.3	33 $\pm$ 4.8	94
HYD-2	1 $\times$ 10 $^{-4}$	511 $\pm$ 1.7	146 $\pm$ 3.8	71 $\pm$ 5.6	208 $\pm$ 5.8	63
	5 $\times$ 10 $^{-4}$	505 $\pm$ 0.5	136 $\pm$ 5.6	77 $\pm$ 8.2	168 $\pm$ 6.7	70
	1 $\times$ 10 $^{-3}$	503 $\pm$ 0.6	139 $\pm$ 5.9	74 $\pm$ 4.4	124 $\pm$ 3.6	78
	5 $\times$ 10 $^{-3}$	500 $\pm$ 0.8	144 $\pm$ 6.7	72 $\pm$ 3.9	89 $\pm$ 4.3	84

Due to the synergistic effect of molecular properties of these inhibitors, it can be assumed that tested molecules adsorbed on the surface, thus preventing both anodic and cathodic processes. Another interesting remark from the results is the remarked difference in the percentage of inhibition efficiency for both inhibitors at the same concentrations. Results from earlier studies demonstrated a consistent and robust association between the unique characteristics of organic molecules and their protection performances. Herein, it is important to mention that the molecular structures as presented above in Figure 1 are different in terms of the number of functional groups as well as the structure size of each molecule. The HYD-1 molecule has three benzene rings, acyl, and an imine substituent, as well as three electron-donating methoxy groups. Thus, it can be concluded that the difference in the

inhibition efficiency is due to all these functional properties of HYD-1, demonstrating the powerful effect of electron-donating properties on the inhibition efficiency.

### 3.3. Electrochemical Impedance Spectroscopy (EIS) Study

#### 3.3.1. Concentration Effect

In Figures 5 and 6, Nyquist and Bode diagrams for the steel electrode are shown with a range of concentrations of the two compounds in 1.0 M HCl at 303 K. In the case of the Nyquist impedance plots, they represent the imaginary component of the plotted impedance as a function of the real component. In contrast, the Bode plots show the logarithm of the impedance modulus  $|Z|$  and phase angle as a function of the logarithm of the frequency  $f$ . Based on the following equation, the double-layer electrical capacity ( $C_{dl}$ ) for each inhibitor concentration is calculated [30]:

$$C_{dl} = \sqrt[n]{Q \times R_p^{1-n}} \quad (7)$$

with  $n$  indicating the phase shift that allows an estimation of the surface heterogeneity of mild steel [31–33]. Based on the EIS technique, for the determination of inhibitory efficacy, the following formula is used:

$$E_{EIS}(\%) = \left[ \frac{R_p^{HYD} - R_p^0}{R_p^{HYD}} \right] \times 100 \quad (8)$$

where  $R_p^0$  and  $R_p^{HYD}$  signify the polarization resistance in the blank solution and with the addition of inhibitors, respectively.

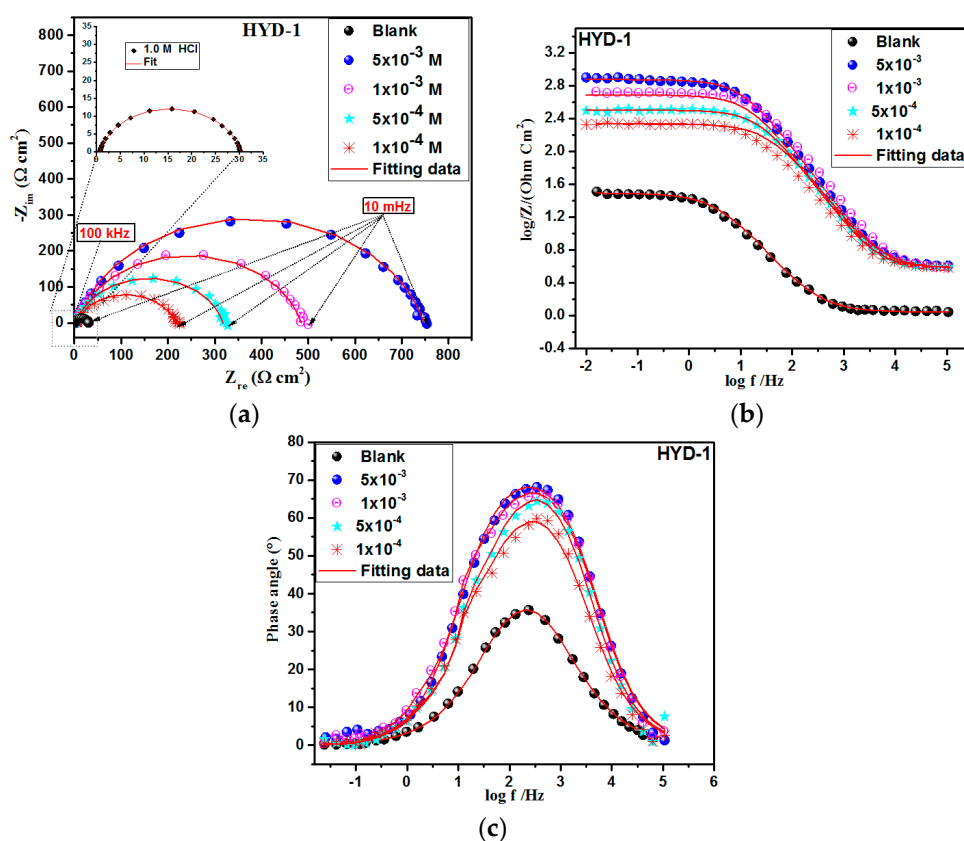


**Figure 5.** Nyquist (a), Bode (b), and phase angle (c) plots of mild steel in 1.0 M HCl with and without various concentrations of HYD-1 inhibitor.

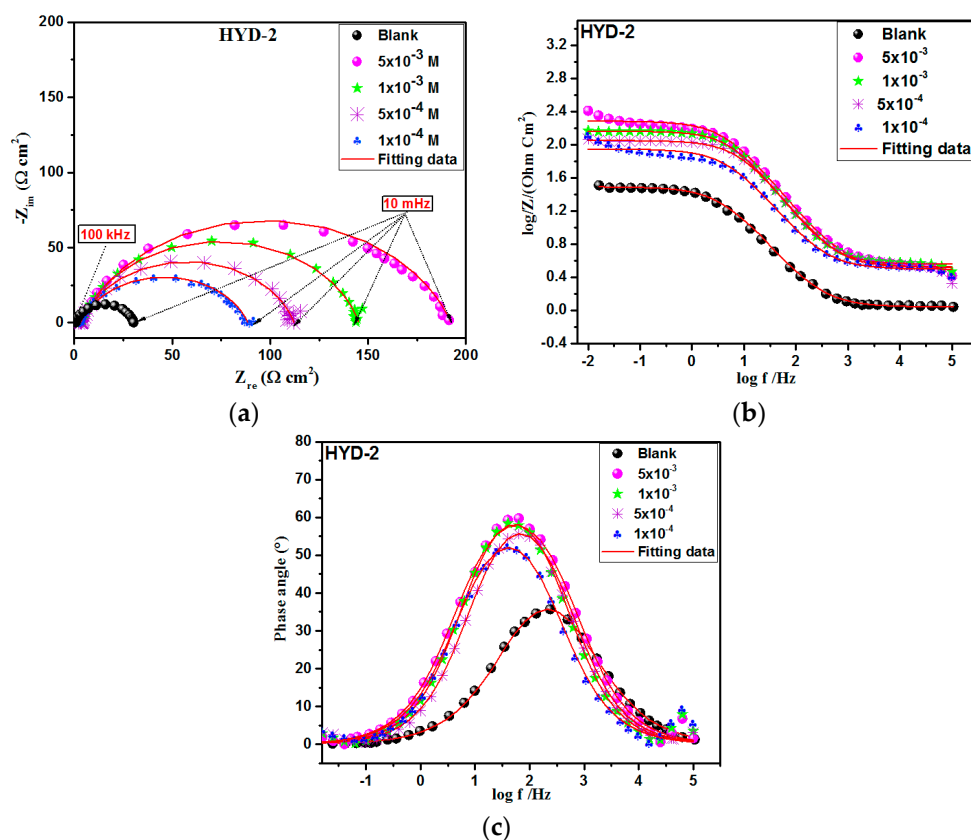


**Figure 6.** Nyquist (a), Bode (b), and phase angle (c) plots of mild steel in 1.0 M HCl with and without various concentrations of HYD-2 inhibitor.

EIS spectra were simulated using the equivalent circuit exposed in Figure 7 to obtain  $R_p$  values that represent the significance of corrosion protection. In a metal/solution interface, the contribution of all resistances, such as film resistance ( $R_f$ ) accumulation resistance ( $R_a$ ), charge transfer resistance ( $R_{ct}$ ), and diffuse layer resistance ( $R_d$ ), must be taken into account. Therefore, the polarization resistance, which is the sum of all resistances, i.e.,  $R_p = R_f + R_{ct} + R_a + R_d$ , was used instead of charge transfer resistance. A detailed explanation has been provided elsewhere [34].

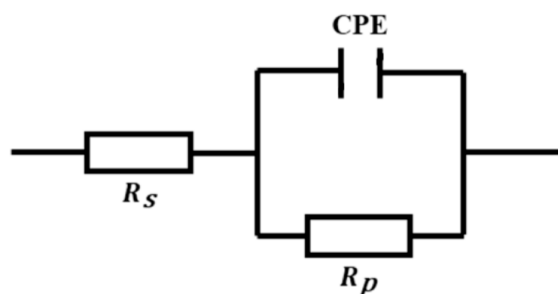


**Figure 7.** Electrochemical equivalent circuit model used to fit and simulate the impedance data.

The corrosion parameters of the studied system such as  $R_p$ ,  $C_{dl}$ , CPE,  $n$ ,  $R_s$ , and  $\eta_{EIS}\%$  are listed in Table 4. Mild steel EIS diagrams obtained without inhibitors (blank) and in the inhibited solutions after 30 min of immersion time show the existence of a single capacitive loop with growing size as the inhibitor concentration rises, indicating that a charge transfer process mainly governs the corrosion of mild steel. It also suggests the enhancement of surface coverage by the inhibitor molecules and the increasing inhibition of mild steel corrosion [2]. According to Table 4, as the concentration of

inhibitors increases,  $R_p$  values increase while  $C_{dl}$  values decrease. These results suggest that adsorption of molecules takes place on the mild steel surface, creating a protective barrier that inhibits the dissolution of the MS in the HCl medium [16,17]. For both inhibitors, we observe that the phase angle values are always higher than that of blank but less than  $-90^\circ$ , indicating the non-ideal capacitor. To conclude, the comparison of inhibitory efficiencies measured by gravimetric and electrochemical methods (polarization and EIS curves) shows good correspondence.

**Table 4.** Electrochemical impedance spectroscopy (EIS) parameters derived after curve fitting in the absence and presence of several concentrations of HYD-1 and HYD-2 at 303 K.

Inhibitor	Concentration (M)	$R_p$ ( $\Omega \text{ cm}^2$ )	$n$	$Q \times 10^{-4}$ ( $\text{S}^n \Omega^{-1} \text{ cm}^{-2}$ )	$C_{dl}$ ( $\mu\text{F cm}^{-2}$ )	Goodness of Fit ( $\chi^2 \times 10^{-3}$ )	$\eta_{\text{EIS}}$ (%)
Blank	1.0	$29 \pm 1.5$	$0.89 \pm 0.005$	$1.761 \pm 0.0025$	92	0.33	-
HYD-1	$1 \times 10^{-4}$	$212 \pm 1.6$	$0.80 \pm 0.004$	$0.742 \pm 0.0031$	26	4.54	86
	$5 \times 10^{-4}$	$313 \pm 1.3$	$0.79 \pm 0.004$	$0.557 \pm 0.0019$	18	4.13	90
	$1 \times 10^{-3}$	$658 \pm 0.9$	$0.83 \pm 0.003$	$0.296 \pm 0.0012$	12	3.86	93
	$5 \times 10^{-3}$	$750 \pm 1.2$	$0.82 \pm 0.005$	$0.179 \pm 0.0024$	7	1.23	96
HYD-2	$1 \times 10^{-4}$	$86 \pm 1.4$	$0.79 \pm 0.007$	$1.173 \pm 0.0085$	34	2.18	65
	$5 \times 10^{-4}$	$108 \pm 1.9$	$0.81 \pm 0.004$	$0.877 \pm 0.0078$	29	6.02	72
	$1 \times 10^{-3}$	$141 \pm 1.6$	$0.83 \pm 0.006$	$0.616 \pm 0.0049$	23	6.18	79
	$5 \times 10^{-3}$	$189 \pm 1.2$	$0.79 \pm 0.001$	$0.583 \pm 0.0077$	17	3.43	84

### 3.3.2. Immersion Time Effect on the Anti-Corrosive Activity of HYD-1

In the field of corrosion inhibition by organic compounds, it is necessary to address the inhibition performance over an extended immersion time. For this purpose, the effect of immersion time on the protection efficiency of HYD-1 was evaluated using EIS diagrams to give more information on the variation of the performance of hydrazone derivatives with the immersion time. EIS curves are shown in Figure 8, while electrochemical characteristics of studied systems are illustrated in Table 5. Data from tests with the presence of the HYD-1 compound can be compared with those obtained without inhibitor. The polarization resistance of MS in the presence of  $5 \times 10^{-3}$  M of HYD-1 decreases as the immersion time increases. However, results in Table 5 show that the inhibition efficiency of HYD-1 remains almost unchanged upon increasing the immersion time. Based on this, it is supposed that this inhibitive performance at longer immersion time is mainly a consequence of a stable inhibitor's adsorption on the steel surface. Again, these results confirm that tested hydrazones could act as effective corrosion inhibitors at different operating conditions.

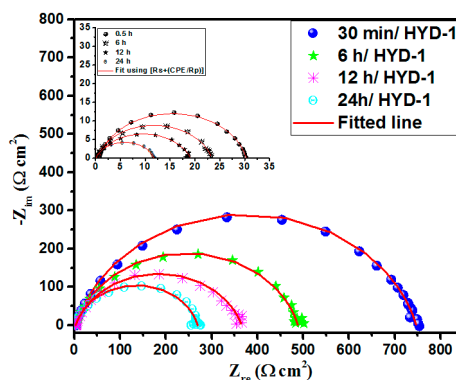


**Figure 8.** Nyquist curves of mild steel in 1.0 M HCl solution without and with  $5 \times 10^{-3}$  M of HYD-1 at various times.

**Table 5.** EIS parameters for mild steel in the absence and presence of HYD-1 at various times.

Inhibitor	Time (h)	$R_p$ ( $\Omega \text{ cm}^2$ )	$n$	$Q \times 10^{-4}$ ( $\text{S}^n \Omega^{-1} \text{cm}^{-2}$ )	$C_{dl}$ ( $\mu\text{F cm}^2$ )	Goodness of Fit ( $\chi^2 \times 10^{-3}$ )	$\eta_{\text{EIS}}$ (%)
Blank	0.5	$29 \pm 1.5$	$0.89 \pm 0.005$	$1.7610 \pm 0.0025$	92	0.33	-
	6	$23 \pm 2.5$	$0.84 \pm 0.007$	$2.5114 \pm 0.0037$	94	2.45	-
	12	$18 \pm 1.7$	$0.83 \pm 0.004$	$2.9866 \pm 0.0084$	102	3.24	-
	24	$12 \pm 2.9$	$0.88 \pm 0.003$	$3.0891 \pm 0.0031$	144	1.14	-
HYD-1	0.5	$750 \pm 1.2$	$0.82 \pm 0.005$	$0.1793 \pm 0.0024$	7	1.23	96
	6	$484 \pm 1.8$	$0.84 \pm 0.002$	$0.3339 \pm 0.0048$	15	2.14	95
	12	$352 \pm 2.7$	$0.81 \pm 0.003$	$0.4994 \pm 0.0017$	19	3.59	94
	24	$265 \pm 1.6$	$0.82 \pm 0.054$	$0.6095 \pm 0.0089$	24	3.12	95

### 3.4. Adsorption Isotherm

Generally, adsorption isotherms are used to obtain information regarding the type of adsorption of organic inhibitor molecules on the mild steel surface during corrosion inhibition process. A variety of adsorption isotherms such as Langmuir, Temkin, and Frumkin were tested. The Langmuir model proved to be the best description (Figure 9a). Its equation is given as follows [35,36]:

$$\frac{C_{\text{inh}}}{\theta} = \frac{1}{K_{\text{ads}}} + C_{\text{inh}} \quad (9)$$

in which  $C_{\text{inh}}$  signifies the inhibitor concentration,  $K_{\text{ads}}$  means the constant of adsorption equilibrium, while  $\theta$  denotes the coverage area.

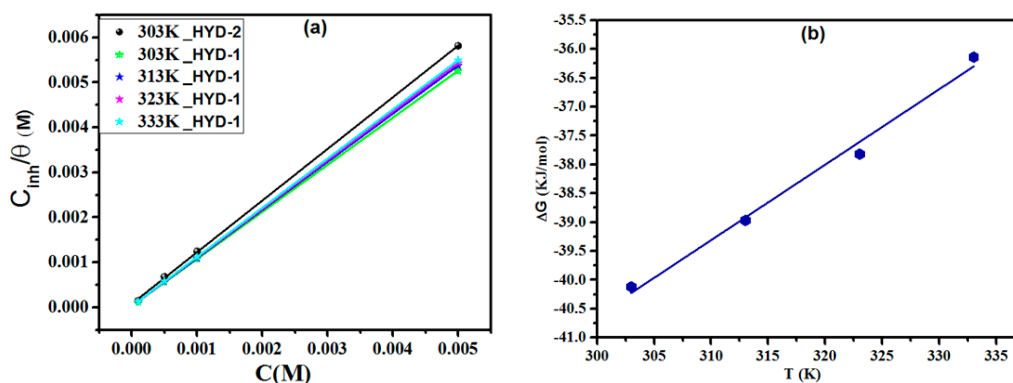


**Figure 9.** (a) Langmuir adsorption isotherm models and (b) the variation of standard Gibbs free energy of HYD-1 with temperature for the adsorption of inhibitor on MS in 1.0 M HCl.

The values of the adsorption coefficient ( $K_{\text{ads}}$ ) were used to determine the values of the standard free adsorption energies ( $\Delta G_{\text{ads}}^{\circ}$ ) from the Van't Hoff equation [32]:

$$K_{\text{ads}} = \frac{1}{55.5} \exp\left(\frac{-\Delta G_{\text{ads}}^{\circ}}{RT}\right) \quad (10)$$

In the above equation, 55.5 denotes the water molar concentration in  $\text{mol L}^{-1}$ ,  $T$  indicates the temperature of the aqueous solution, and  $R$  is the universal gas constant. The adsorption parameters  $\Delta H_{\text{ads}}^{\circ}$  and  $\Delta S_{\text{ads}}^{\circ}$  on the MS surface are computed according to the next relationship [37]:

$$\Delta G_{\text{ads}}^{\circ} = \Delta H_{\text{ads}}^{\circ} - T\Delta S_{\text{ads}}^{\circ} \quad (11)$$

Thermodynamic parameters estimated from Langmuir's plots are tabulated in Table 6. This table shows high negative values of  $\Delta G_{\text{ads}}^{\circ}$ , which is an indication of the marked interaction of the studied molecules with the MS surface and the spontaneity of the adsorption process [36,38–40]. On the other hand,  $\Delta G_{\text{ads}}^{\circ}$  values are between  $-40$  and  $-20$   $\text{kJ mol}^{-1}$ , which indicates that the adsorption is of a mixed type (chemical and physical interactions) [37]. The values of  $\Delta H_{\text{ads}}^{\circ}$  and  $\Delta S_{\text{ads}}^{\circ}$  of HYD-1 were determined from Figure 9b, and results are also presented in Table 6. The negative values of  $\Delta H_{\text{ads}}^{\circ}$  and  $\Delta S_{\text{ads}}^{\circ}$  pretend that the inhibitor's adsorption on metal is perceived essentially as an exothermic reaction, accompanied by a reduction in entropy.

**Table 6.** Thermodynamic parameters of mild steel corrosion in 1.0 M HCl solution with the presence of HYD-1 and HYD-2.

Inhibitor	Temperature (K)	$K_{\text{ads}}$ (L/mol)	$R^2$	$\Delta G_{\text{ads}}^{\circ}$ (kJ/mol)	$\Delta H_{\text{a}}$ (kJ mol <sup>-1</sup> )	$\Delta S_{\text{a}}$ (J mol <sup>-1</sup> K <sup>-1</sup> )
HYD-2	303	12,311	0.999	-33.82	-	-
	303	30,910	0.999	-40.12		
HYD-1	313	37,315	0.999	-38.97	-79.88	-13.09
	323	36,491	0.999	-37.82		
	333	35,675	0.999	-36.14		

### 3.5. Surface Morphological Study

SEM analysis is an effective method for studying the morphology of mild steel surface after being immersed in various mediums. This technique is particularly useful to characterize the development of a protective organic layer on the surface that allows a high degree of inhibition resistance. Figure 10a,b illustrates the surface morphology of processed mild steel surfaces immersed for 24 h in two different solutions; non-inhibited solution and that with  $5 \times 10^{-3}$  M of HYD-1 inhibitor. As Figure 10 shows, there is a significant difference between the two SEM micrographs. From Figure 10a, we can see that without inhibitors, the MS surface is highly corroded and contains internal corrosion damage, which is due to rapid corrosion attack in the acid solution; hence, the MS surface becomes inhomogeneous and rough. However, Figure 10b shows that with the presence of the HYD-1 inhibitor, the damage of the MS surface is significantly reduced, meaning that the surface morphology is more protected due to the HYD-1 adsorption onto the mild steel surface.

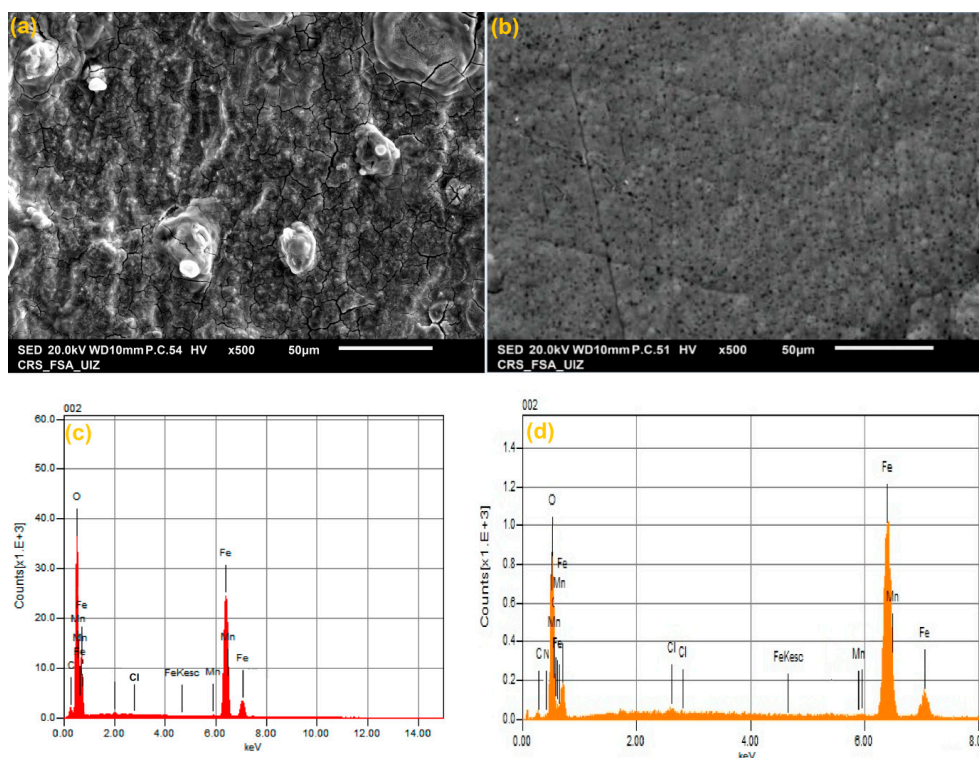


**Figure 10.** SEM and EDX photographs of mild steel specimens after 24 h of immersion in 1.0 M HCl solution in the absence (a,c) and the presence of  $5 \times 10^{-3}$  M of HYD-1 (b,d).

Furthermore, to identify the elemental composition of the MS samples before and after the addition of studied inhibitor, EDX analysis was performed and analyzed. It can be observed that MS in uninhibited solution (Figure 10c) contains a large percentage of iron, oxygen, and carbon atoms. Comparing this percentage shown in the blank spectrum with the spectrum of the sample in the presence of HYD-1 (Figure 10d), it is observed that the peaks of Cl and O are significantly reduced, which means a decrease in the density of corrosion active sites. Moreover, with the introduction of HYD-1, a new peak of nitrogen appeared, which confirms the presence of our studied inhibitor on the MS surface. All these observations indicate that the corrosion of MS is reduced after the addition of the HYD-1 molecule. These results are not surprising bearing in mind the presence of aromatic rings and the hydrazide group, which facilitates the adsorption of the tested molecule at the surface, and therefore, ensuring remarkable prevention against corrosion. Surface characterization analysis supports the results obtained from gravimetric and electrochemical tests.

#### 4. Conclusions

The corrosion inhibition effect of (E)-N'-(2,4-dimethoxybenzylidene)-2-(6-methoxynaphthalen-2-yl)propanehydrazide (HYD-1) and N'-cyclohexylidene-2-(6-methoxynaphthalen-2-yl)propanehydrazide (HYD-2) on mild steel corrosion in 1.0 M HCl solution was investigated. In summary, the obtained results clearly showed that the HYDs acted as excellent corrosion inhibitors. Further, the adsorption mechanism in terms of adsorption type, temperature effect, the influence of immersion time, and surface morphological characterization was also discussed. It can be concluded that the inhibitory efficacy of HYDs depended on the nature of the substituents and HYD-1 presented better inhibitive performances than HYD-2 owing to its functional properties (molecular size and electron-donating groups). Concerning the temperature effect on the inhibition efficiency, it can be concluded that no significant decrease in the protection efficiency under different temperatures ranging from 303 K to 333 K was observed. Moreover, the performance of inhibition was unchanged with increasing immersion time. Electrochemical results showed that HYDs acted as mixed-type inhibitors and led

to an increase in the polarization resistance even at a low concentration. Furthermore, the HYDs adsorption on the MS surface followed the Langmuir model, and it occurs via a combination of chemical and physical interactions. The higher corrosion inhibition by tested compounds is due to the synergistic effect of different substituent groups present in the studied molecules, which will be studied in detail in future research in which we will focus on the theoretical study of tested hydrazone derivatives.

**Supplementary Materials:** The following are available online at <http://www.mdpi.com/2079-6412/10/7/640/s1>, Scheme 1: General procedure for the synthesis of hydrazones (3,4).

**Author Contributions:** Conceptualization, methodology, supervision, and writing—review and editing, H.L. and I.-M.C.; data curation, formal analysis, and writing—original draft preparation, A.C., M.C., and H.L.; investigation and writing—review and editing, M.R.A.-H. and S.M.; project administration, funding acquisition, and writing—review and editing, I.H.A.; All authors have read and agreed to the published version of the manuscript.

**Funding:** This research was funded by the Deanship of Scientific Research at King Khalid University, grant number R.G.P. 2/94/41.

**Acknowledgments:** The authors extend their appreciation to the Deanship of Scientific Research at King Khalid University for funding this research through research groups program under grant number R.G.P. 2/94/41.

**Conflicts of Interest:** The authors declare no conflict of interest.

## References

1. Bentiss, F.; Gassama, F.; Barbry, D.; Gengembre, L.; Vezin, H.; Lagrenée, M.; Traisnel, M. Enhanced corrosion resistance of mild steel in molar hydrochloric acid solution by 1, 4-bis (2-pyridyl)-5H-pyridazino [4, 5-b] indole: Electrochemical, theoretical and XPS studies. *Appl. Surf. Sci.* **2006**, *252*, 2684–2691. [CrossRef]
2. Solmaz, R. Investigation of adsorption and corrosion inhibition of mild steel in hydrochloric acid solution by 5-(4-Dimethylaminobenzylidene)rhodanine. *Corros. Sci.* **2014**, *79*, 169–176. [CrossRef]
3. Lgaz, H.; Saha, S.K.; Chaouiki, A.; Bhat, K.S.; Salghi, R.; Banerjee, P.; Ali, I.H.; Khan, M.I.; Chung, I.-M. Exploring the potential role of pyrazoline derivatives in corrosion inhibition of mild steel in hydrochloric acid solution: Insights from experimental and computational studies. *Constr. Build. Mater.* **2020**, *233*, 117320. [CrossRef]
4. Ouici, H.B.; Benali, O.; Guendouzi, A. Experimental and quantum chemical studies on the corrosion inhibition effect of synthesized pyrazole derivatives on mild steel in hydrochloric acid. *Res. Chem. Intermed.* **2016**, *42*, 7085–7109. [CrossRef]
5. Bentiss, F.; Lagrenée, M.; Traisnel, M.; Hornez, J. The corrosion inhibition of mild steel in acidic media by a new triazole derivative. *Corros. Sci.* **1999**, *41*, 789–803. [CrossRef]
6. Chugh, B.; Singh, A.K.; Chaouiki, A.; Salghi, R.; Thakur, S.; Pani, B. A comprehensive study about anti-corrosion behaviour of pyrazine carbohydrazone: Gravimetric, electrochemical, surface and theoretical study. *J. Mol. Liq.* **2020**, *299*, 112160. [CrossRef]
7. Verma, C.; Olasunkanmi, L.; Obot, I.; Ebenso, E.E.; Quraishi, M. 5-Arylpymido-[4, 5-b] quinoline-diones as new and sustainable corrosion inhibitors for mild steel in 1 M HCl: A combined experimental and theoretical approach. *RSC Adv.* **2016**, *6*, 15639–15654. [CrossRef]
8. Rani, B.; Basu, B.B.J. Green inhibitors for corrosion protection of metals and alloys: An overview. *Int. J. Corros.* **2012**, *2012*. [CrossRef]
9. Lgaz, H.; Zehra, S.; Albayati, M.; Toumiat, K.; El Aoufir, Y.; Chaouiki, A.; Salghi, R.; Ali, I.H.; Khan, M.; Chung, I. Corrosion Inhibition of Mild Steel in 1.0 M HCl by two Hydrazone Derivatives. *Int. J. Electrochem. Sci.* **2019**, *14*, 6667–6681.
10. Chaouiki, A.; Lgaz, H.; Zehra, S.; Salghi, R.; Chung, I.-M.; El Aoufir, Y.; Bhat, K.S.; Ali, I.H.; Gaonkar, S.L.; Khan, M.I. Exploring deep insights into the interaction mechanism of a quinazoline derivative with mild steel in HCl: Electrochemical, DFT, and molecular dynamic simulation studies. *J. Adhes. Sci. Technol.* **2019**, *33*, 921–944. [CrossRef]
11. Chafiq, M.; Chaouiki, A.; Lgaz, H.; Salghi, R.; Bhaskar, K.V.; Marzouki, R.; Bhat, K.S.; Ali, I.H.; Khan, M.I.; Chung, I.-M. Inhibition performances of spirocyclopropane derivatives for mild steel protection in HCl. *Mater. Chem. Phys.* **2020**, *243*, 122582. [CrossRef]

12. Chafiq, M.; Chaouiki, A.; Lgaz, H.; Salghi, R.; Bhaskar, K.V.; Thakur, P.S.; Bhat, K.S.; Ali, I.H.; Khan, M.; Chung, I.M. New spirocyclopropane derivatives: Synthesis and evaluation of their performances toward corrosion inhibition of mild steel in acidic media. *Res. Chem. Intermed.* **2020**, *46*, 2881–2918. [[CrossRef](#)]
13. Chaouiki, A.; Lgaz, H.; Salghi, R.; Chafiq, M.; Oudda, H.; Bhat, K.; Cretescu, I.; Ali, I.; Marzouki, R.; Chung, I. Assessing the impact of electron-donating-substituted chalcones on inhibition of mild steel corrosion in HCl solution: Experimental results and molecular-level insights. *Colloids Surf. Physicochem. Eng. Asp.* **2020**, *588*, 124366. [[CrossRef](#)]
14. Mamatha, N.; Babu, N.S.; Mukkanti, K.; Pal, S. 2-(6-Methoxynaphthalen-2-yl) propionic acid (1, 3-dimethylbutylidene) hydrazide. *Molbank* **2011**, *2011*, M741. [[CrossRef](#)]
15. Almasirad, A.; Tajik, M.; Bakhtiari, D.; Shafiee, A.; Abdollahi, M.; Zamani, M.J.; Khorasani, R.; Esmaily, H. Synthesis and analgesic activity of N-arylhydrazone derivatives of mefenamic acid. *J. Pharm. Pharm. Sci.* **2005**, *8*, 419–425. [[PubMed](#)]
16. Lgaz, H.; Chaouiki, A.; Albayati, M.R.; Salghi, R.; El Aoufir, Y.; Ali, I.H.; Khan, M.I.; Mohamed, S.K.; Chung, I.-M. Synthesis and evaluation of some new hydrazones as corrosion inhibitors for mild steel in acidic media. *Res. Chem. Intermed.* **2019**, *45*, 2269–2286. [[CrossRef](#)]
17. Lgaz, H.; Chung, I.-M.; Albayati, M.R.; Chaouiki, A.; Salghi, R.; Mohamed, S.K. Improved corrosion resistance of mild steel in acidic solution by hydrazone derivatives: An experimental and computational study. *Arab. J. Chem.* **2020**, *13*, 2934–2954. [[CrossRef](#)]
18. ASTM G31-72 Standard Practice for Laboratory Immersion Corrosion Testing of Metals; ASTM: Philadelphia, PA, USA, 1995.
19. Dehghani, A.; Bahlakeh, G.; Ramezanzadeh, B.; Ramezanzadeh, M. A combined experimental and theoretical study of green corrosion inhibition of mild steel in HCl solution by aqueous Citrullus lanatus fruit (CLF) extract. *J. Mol. Liq.* **2019**, *279*, 603–624. [[CrossRef](#)]
20. Quraishi, M.A.; Singh, A.; Singh, V.K.; Yadav, D.K.; Singh, A.K. Green approach to corrosion inhibition of mild steel in hydrochloric acid and sulphuric acid solutions by the extract of *Murraya koenigii* leaves. *Mater. Chem. Phys.* **2010**, *122*, 114–122. [[CrossRef](#)]
21. Verma, C.B.; Quraishi, M.; Singh, A. 2-Aminobenzene-1, 3-dicarbonitriles as green corrosion inhibitor for mild steel in 1 M HCl: Electrochemical, thermodynamic, surface and quantum chemical investigation. *J. Taiwan Inst. Chem. Eng.* **2015**, *49*, 229–239. [[CrossRef](#)]
22. Wadhvani, P.M.; Ladha, D.G.; Panchal, V.K.; Shah, N.K. Enhanced corrosion inhibitive effect of p-methoxybenzylidene-4, 4'-dimorpholine assembled on nickel oxide nanoparticles for mild steel in acid medium. *RSC Adv.* **2015**, *5*, 7098–7111. [[CrossRef](#)]
23. Yadav, M.; Gope, L.; Kumari, N.; Yadav, P. Corrosion inhibition performance of pyranopyrazole derivatives for mild steel in HCl solution: Gravimetric, electrochemical and DFT studies. *J. Mol. Liq.* **2016**, *216*, 78–86. [[CrossRef](#)]
24. Yadav, D.K.; Chauhan, D.; Ahamad, I.; Quraishi, M. Electrochemical behavior of steel/acid interface: Adsorption and inhibition effect of oligomeric aniline. *RSC Adv.* **2013**, *3*, 632–646. [[CrossRef](#)]
25. Li, X.; Deng, S.; Fu, H. Three pyrazine derivatives as corrosion inhibitors for steel in 1.0 M H<sub>2</sub>SO<sub>4</sub> solution. *Corros. Sci.* **2011**, *53*, 3241–3247. [[CrossRef](#)]
26. Chaouiki, A.; Lgaz, H.; Chung, I.-M.; Ali, I.; Gaonkar, S.L.; Bhat, K.; Salghi, R.; Oudda, H.; Khan, M. Understanding corrosion inhibition of mild steel in acid medium by new benzonitriles: Insights from experimental and computational studies. *J. Mol. Liq.* **2018**, *266*, 603–616. [[CrossRef](#)]
27. Kowsari, E.; Arman, S.; Shahini, M.; Zandi, H.; Ehsani, A.; Naderi, R.; PourghasemiHanza, A.; Mehdipour, M. In situ synthesis, electrochemical and quantum chemical analysis of an amino acid-derived ionic liquid inhibitor for corrosion protection of mild steel in 1M HCl solution. *Corros. Sci.* **2016**, *112*, 73–85. [[CrossRef](#)]
28. Yüce, A.O.; Mert, B.D.; Kardaş, G.; Yazıcı, B. Electrochemical and quantum chemical studies of 2-amino-4-methyl-thiazole as corrosion inhibitor for mild steel in HCl solution. *Corros. Sci.* **2014**, *83*, 310–316. [[CrossRef](#)]
29. Saini, N.; Kumar, R.; Lgaz, H.; Salghi, R.; Chung, I.-M.; Kumar, S.; Lata, S. Minified dose of urispas drug as better corrosion constraint for soft steel in sulphuric acid solution. *J. Mol. Liq.* **2018**, *269*, 371–380. [[CrossRef](#)]
30. Zhang, Z.; Tian, N.; Huang, X.; Shang, W.; Wu, L. Synergistic inhibition of carbon steel corrosion in 0.5 M HCl solution by indigo carmine and some cationic organic compounds: Experimental and theoretical studies. *RSC Adv.* **2016**, *6*, 22250–22268.

31. Quraishi, M.; Sardar, R.; Jamal, D. Corrosion inhibition of mild steel in hydrochloric acid by some aromatic hydrazides. *Mater. Chem. Phys.* **2001**, *71*, 309–313. [[CrossRef](#)]
32. Bentiss, F.; Traisnel, M.; Chaibi, N.; Mernari, B.; Vezin, H.; Lagrenee, M. 2, 5-Bis (n-methoxyphenyl)-1, 3, 4-oxadiazoles used as corrosion inhibitors in acidic media: Correlation between inhibition efficiency and chemical structure. *Corros. Sci.* **2002**, *44*, 2271–2289. [[CrossRef](#)]
33. Wang, X.; Yang, H.; Wang, F. A cationic gemini-surfactant as effective inhibitor for mild steel in HCl solutions. *Corros. Sci.* **2010**, *52*, 1268–1276. [[CrossRef](#)]
34. Solmaz, R.; Kardaş, G.; Çulha, M.; Yazıcı, B.; Erbil, M. Investigation of adsorption and inhibitive effect of 2-mercaptothiazoline on corrosion of mild steel in hydrochloric acid media. *Electrochimica Acta* **2008**, *53*, 5941–5952. [[CrossRef](#)]
35. Ganjali, M.; Norouzi, P.; Alizadeh, T.; Adib, M. Application of 8-amino-N-(2-hydroxybenzylidene) naphthyl amine as a neutral ionophore in the construction of a lanthanum ion-selective sensor. *Anal. Chim. Acta* **2006**, *576*, 275–282. [[CrossRef](#)]
36. Li, X.; Deng, S.; Lin, T.; Xie, X.; Du, G. 2-Mercaptopyrimidine as an effective inhibitor for the corrosion of cold rolled steel in HNO<sub>3</sub> solution. *Corros. Sci.* **2017**, *118*, 202–216. [[CrossRef](#)]
37. Umoren, S.A.; Eduok, U.M.; Solomon, M.M.; Udoh, A.P. Corrosion inhibition by leaves and stem extracts of *Sida acuta* for mild steel in 1 M H<sub>2</sub>SO<sub>4</sub> solutions investigated by chemical and spectroscopic techniques. *Arab. J. Chem.* **2016**, *9*, S209–S224. [[CrossRef](#)]
38. Aljourani, J.; Raeissi, K.; Golozar, M. Benzimidazole and its derivatives as corrosion inhibitors for mild steel in 1M HCl solution. *Corros. Sci.* **2009**, *51*, 1836–1843. [[CrossRef](#)]
39. Gurudatt, D.M.; Mohana, K.N. Synthesis of new pyridine based 1, 3, 4-oxadiazole derivatives and their corrosion inhibition performance on mild steel in 0.5 M hydrochloric acid. *Ind. Eng. Chem. Res.* **2014**, *53*, 2092–2105. [[CrossRef](#)]
40. Mahdavian, M.; Ashhari, S. Corrosion inhibition performance of 2-mercaptobenzimidazole and 2-mercaptobenzoxazole compounds for protection of mild steel in hydrochloric acid solution. *Electrochimica Acta* **2010**, *55*, 1720–1724. [[CrossRef](#)]



© 2020 by the authors. Licensee MDPI, Basel, Switzerland. This article is an open access article distributed under the terms and conditions of the Creative Commons Attribution (CC BY) license (<http://creativecommons.org/licenses/by/4.0/>).